5-1-1988

Effects of Eddy Viscosity and Thermal Conduction and Coriolis Force in the Dynamics of Gravity Wave Driven Fluctuations in the OH Nightglow

Michael P. Hickey Ph.D.
Embry-Riddle Aeronautical University, hicke0b5@erau.edu

JOURNAL OF GEOPHYSICAL RESEARCH, VOL. 93, NO. A5, PAGES 4077–4088, MAY 1, 1988

Effects of Eddy Viscosity and Thermal Conduction and Coriolis Force in the Dynamics of Gravity Wave Driven Fluctuations in the OH Nightglow

M. P. HICKEY

Universities Space Research Association, NASA Marshall Space Flight Center, Huntsville, Alabama

Recently, Walterscheid et al. (1987) have described a dynamical-chemical model of wave-driven fluctuations in the OH nightglow which incorporated a five-reaction photochemical scheme and the dynamics of linearized acoustic-gravity waves in an isothermal, motionless atmosphere. The intensity oscillation (δI) about the time-averaged intensity (I_0) and the temperature oscillation (δT) about the time-averaged temperature (T_0) were related by means of the complex ratio $\eta \equiv (\delta I/I_0)/(\delta T/T_0)$. One of the main conclusions of their work was that the inclusion of dynamical effects is absolutely essential for a valid assessment of η at any wave period. In this paper the model of Walterscheid et al. (1987) is modified to include in the gravity wave dynamics the effects of eddy viscosity, eddy thermal conduction, and Coriolis force (with the shallow atmosphere approximation), and calculations are performed for the same nominal case as used by these previous authors (i.e., $\lambda_x = 100$ km and atmospheric conditions pertinent to 83 km altitude), but only gravity wave periods are considered. It is found that for wave periods greater than some 2 or 3 hours the value of η is greatly modified by the inclusion of eddy thermal conduction. Although when acting alone the eddy viscosity is relatively unimportant, it significantly modifies the results when acting in conjunction with the eddy thermal conduction. The inclusion of the Coriolis force is found to be insignificant at any wave period. Although it is for the longest-period waves that the values of η are most modified by the inclusion of dissipation, this dissipation may be severe enough to place an observational constraint on such waves. Results of Walterscheid et al. (1987) suggest that η is virtually independent of horizontal wavelength (λ_x), but it is indicated here that the inclusion of dissipation is likely to make η highly dependent on λ_x and to complicate comparisons which have been made between observation and theory. The effects of varying the Prandtl number are also discussed.

INTRODUCTION

Acoustic-gravity waves upset the chemical equilibrium in the upper mesosphere, thus modulating the emission intensity of the hydroxyl (OH) nightglow. These waves are also responsible for fluctuations in kinetic temperature which, due to the high collision frequency in the mesosphere and the consequent maintenance of local thermodynamic equilibrium, can be measured in the rotational temperature of the OH emissions. A useful parameter was introduced by *Krassovsky* [1972] to relate the oscillation in intensity (δI) to that in the rotational temperature (δT), and is given by

$$\eta \equiv (\delta I/I_0)/(\delta T/T_0)$$

where a zero subscript refers to the undisturbed variable. This parameter was shown by *Walterscheid et al.* [1987] to be a complex quantity depending on wave period, height of the OH emission layer, and the value of the atomic oxygen scale height. Measurements of the magnitude and phase of η have been made by *Hecht et al.* [1987] for gravity waves and by *Sivjee et al.*, [1987] for a gravity wave and possibly also a semidiurnal pseudotide (a phenomenon discussed by *Walterscheid et al.* [1986]).

A recent comprehensive model to describe fluctuations in the OH nightglow has been presented by *Walterscheid et al.* [1987]. This model included chemistry as well as the dynamics of acoustic-gravity waves, and importantly, the model was an Eulerian one. However, the dynamics used the most basic acoustic-gravity wave theory of *Hines* [1960] and took no account of either the Earth's rotation or of dissipation, effects which are likely to be important for some waves in the mesosphere (see, for example, papers by *Ebel* [1984], *Fritts* [1984], *Walterscheid* [1981], and *Weinstock* [1984], all of which describe dissipative effects on gravity wave dynamics in the mesosphere, and *Smith et al.* [1986], whose observation of an inertiogravity wave demonstrated the importance of the Coriolis force on some gravity waves in the mesosphere). Note, however, that *Walterscheid and Schubert* [1987] extended this model to include tidal dynamics by using the tidal equation and the equivalent depths of the various tidal modes, so that the Coriolis force was implicitly included in that particular analysis.

Here the model of *Walterscheid et al.* [1987] is modified so that the dynamics include the effects of both eddy thermal conduction and viscosity as well as the Coriolis force, which is included using the shallow atmosphere approximation. The basic equations used to accomplish this along with the underlying assumptions, as well as the modified dispersion equation, can be found in the work by *Hickey and Cole* [1987]. Comparisons are performed both with and without these added effects (in various combinations) for the nominal case which was studied by *Walterscheid et al.* [1987], which corresponds to an emission altitude of 83 km and a horizontal wavelength of 100 km. For this particular wavelength the results are found to be unaffected by the inclusion of the Coriolis force at any wave period and so are not included here, though the Coriolis terms are still retained in the equations.

THEORY

The theory and model formalism used here follows very closely that of *Walterscheid et al.* [1987], and so only the main features of this model will be described here. For completeness, however, most of their equations will be included.

The chemical reactions describing the production and loss

Paper number 7A9188.
0148-0227/88/007A-9188$05.00

TABLE 1. Expressions for the Reaction Rates in Table 2

Reaction Rate	Formula
k_2	$1.0 \times 10^{-34} \exp(510/T)$ cm^6/s
k_7	4×10^{-11}, cm^3/s
k_9	$1.4 \times 10^{-10} \exp(-470/T)$, cm^3/s
k_{10}	$2.1 \times 10^{-32} \exp(290/T)$, cm^6/s
k_{11}	4×10^{-11} cm^3/s

From *Winick* [1983].

of OH are

$$H + O_3 \rightarrow OH + O_2 \qquad (k_9) \qquad (1)$$

$$O + HO_2 \rightarrow OH + O_2 \qquad (k_{11}) \qquad (2)$$

$$O + OH \rightarrow O_2 + H \qquad (k_7) \qquad (3)$$

$$O + O_2 + M \rightarrow O_3 + M \qquad (k_2) \qquad (4)$$

$$H + O_2 + M \rightarrow HO_2 + M \qquad (k_{10}) \qquad (5)$$

Here molecular oxygen and $M(O_2 + N_2)$ are assumed to be part of the background major gas. The reaction rates indicated in (1)–(5) are given in Table 1.

The continuity equation is used to determine the number density n of any of the minor species, each of which is assumed to have the same temperature T and velocity $\mathbf{v}$ as the background major gas. Linearization of this equation yields

$$\frac{\partial n}{\partial t} = \mathscr{P} - \mathscr{L} - \frac{dn_0}{dz} w - n_0 \nabla \cdot \mathbf{v} \qquad (6)$$

where z is altitude, w the vertical component of velocity, and $\mathscr{P}$ and $\mathscr{L}$ are the volumetric production and loss rates, respectively, of the minor constitutents by chemical reactions (these chemical production and loss terms are listed in Table 2.). Unsubscripted variables refer to the wave, while those subscripted with a zero refer to the unperturbed basic state. Note that there are five equations of the form of (6) to describe the time evolution of $n(OH)$, $n(O_3)$, $n(H)$, $n(O)$, and $n(HO_2)$. If the perturbations are due to plane waves propagating in the x-z plane (x is the horizontal coordinate), then one may write

$$(n, T, \mathbf{v}, \cdots) = [\hat{n}(z), \hat{T}(z), \hat{\mathbf{v}}(z), \cdots] \exp i(\omega t - k_x x) \qquad (7)$$

where ω is the wave angular frequency and k_x is the horizontal wave number. Substitution of (7) into (6) then yields

$$i\omega\hat{n} = \hat{\mathscr{P}} - \hat{\mathscr{L}} - \frac{dn_0}{dz} \hat{w} - n_0 \nabla \cdot \hat{\mathbf{v}} \qquad (8)$$

Internal gravity wave theory is used to relate $\hat{w}$, $\nabla \cdot \hat{\mathbf{v}}$, and $\hat{n}(M)$ to $\hat{T}$. The analysis now departs from that of Walterscheid et al. [1987]. Instead of employing the simplified gravity wave equations of *Hines* [1960], the theory is extended to include the dynamical effects of internal gravity waves propagating in a viscous, thermally conducting and rotating (though windless) isothermal atmosphere. For this purpose the equations and notation of *Hickey and Cole* [1987] are employed, neglecting the effects of ion drag. The Coriolis force is included using the shallow atmosphere approximation (see *Hickey and Cole* [1987] for an explanation of the validity of this). One of the effects of viscosity and thermal conduction is to dissipate wave energy, and hence at times they will be collectively termed "the effects of dissipation."

Without loss of generality, phase propagation is assumed to be in the meridional (x) direction. The basic altitude dependence of wave variables appearing in (7) is written as

$$\frac{\hat{n}}{n_0} = \frac{\hat{\rho}}{\rho_0}, \hat{\mathbf{v}}, \hat{T} \propto \exp(1/2H - ik_z)z \qquad (9)$$

In this case the nondimensional equations of momentum, continuity, and energy become (after first using the ideal gas equation to eliminate the pressure)

$$(\phi + \eta')\hat{u}_1 - ic\hat{v}_1 + \eta'(\kappa - 3i\alpha)\hat{w} + \frac{\hat{\rho}}{\rho_0} + \frac{\hat{T}}{T_0} = 0 \qquad (10)$$

$$\hat{v}_1 = -ic\phi^{-1}\hat{u}_1 \qquad (11)$$

$$\eta'(\kappa + 2i\alpha)\hat{u}_1 + [\eta'(4R - 1) - \beta']\hat{w}_1 + \kappa\frac{\hat{\rho}}{\rho_0} + (\kappa - i\alpha)\frac{\hat{T}}{T_0} = 0 \qquad (12)$$

$$\hat{u}_1 + (\kappa - i\alpha)\hat{w}_1 = \frac{\hat{\rho}}{\rho_0} \qquad (13)$$

$$\hat{u}_1 + \kappa\hat{w}_1 = \left\{\frac{1}{(\gamma - 1)} - \nu R\right\}\frac{\hat{T}}{T_0} \qquad (14)$$

where ρ is mass density, v is zonal velocity, and the velocity components have been nondimensionalized by multiplication of k_x/ω, e.g., $\hat{u}_1 = k_x\hat{u}/\omega$.

Also,

$$\begin{aligned} \phi &= 3\eta' R - \beta' & R &= \kappa^2 - i\alpha\kappa + 1 \\ \kappa &= \frac{k_z + (i/2H)}{k_x} & \alpha &= \frac{1}{k_x H} \\ \beta' &= \frac{\omega^2}{gHk_x^2} & \eta' &= \frac{i\omega\mu}{3p_0} \\ \nu &= \frac{i\lambda T_0 k_x^2}{\omega p_0} & c &= \frac{f\omega}{gHk_x^2} \\ f &= 2\Omega \sin\theta \end{aligned} \qquad (15)$$

Here H is the pressure scale height, p_0 is the unperturbed pressure, g is the acceleration due to gravity, k_z is the complex

TABLE 2. Rates of Volumetric Production $\mathscr{P}$ and Loss $\mathscr{L}$ of Minor Constituents by the Chemical Reactions of (1)–(5)

Minor Species	$\mathscr{P}$	$\mathscr{L}$
OH	$k_9 n(H)n(O_3) + k_{11} n(O)n(HO_2)$	$k_7 n(O)n(OH)$
O_3	$k_2 n(O)n(O_2)n(M)$	$k_9 n(H)n(O_3)$
H	$k_7 n(O)n(OH)$	$k_9 n(H)n(O_3) + k_{10} n(H)n(O_2)n(M)$
O		$n(O)\{k_7 n(OH) + k_2 n(O_2)n(M) + k_{11} n(HO_2)\}$
HO_2	$k_{10} n(H)n(O_2)n(M)$	$k_{11} n(O)n(HO_2)$

vertical wave number, μ is the coefficient of (eddy) viscosity, λ is the coefficient of (eddy) thermal conduction, f is the Coriolis parameter, θ is the latitude, and Ω ($= 7.29 \times 10^{-5}\ s^{-1}$) is the Earth's angular frequency. The vertical wave number can be obtained from use of the quartic dispersion equation of *Hickey and Cole* [1987].

The form of the energy equation (14) adopted here with eddy thermal conduction replacing molecular thermal conduction is, according to *Schoeberl et al.* [1983], physically meaningful only when it describes the transport of potential temperature, and is sufficiently accurate when formulated in terms of the temperature if the vertical wave number of the disturbance [Re (k_z)] is large, i.e., [Re (k_z)] > $1/H$. As it transpires, the effects of the eddy thermal conduction are most important for waves of short vertical wavelength, so that the use of eddy thermal conduction in equation (14) to describe the transport of temperature is a good approximation to be used in this study.

To obtain $\nabla \cdot \hat{\mathbf{v}}$ in terms of $\hat{T}/T_0$, one can simply use the energy equation (14), which gives (remembering that $\hat{\mathbf{v}}_1 = k_x\hat{\mathbf{v}}/\omega$ and noting that $\partial/\partial z = -ik_x\kappa$)

$$\nabla \cdot \hat{\mathbf{v}} = f_1 \frac{\hat{T}}{T_0} \tag{16}$$

where

$$f_1 = i\omega\left\{\nu R - \frac{1}{(\gamma - 1)}\right\} \tag{17}$$

To obtain both $\hat{w}$ and $\hat{\rho}/\rho_0$ in terms of $\hat{T}/T_0$, one needs to solve the set of equations (10)–(14). The process involved is quite straightforward and leads to

$$\hat{w} = f_2\, \hat{T}/T_0 \tag{18}$$

$$f_2 = \frac{(\omega/k_x)\{x_1 + x_3[\nu R - (\gamma - 1)^{-1}]\}}{(x_2 - i\alpha x_3)} \tag{19}$$

$$\hat{\rho}/\rho_0 = f_3\, \hat{T}/T_0 \tag{20}$$

$$f_3 = \frac{\{i\alpha x_1 + x_2[\nu R - (\gamma - 1)^{-1}]\}}{(i\alpha x_3 - x_2)} \tag{21}$$

$$x_1 = (i\alpha - \kappa)(\phi - c^2\phi^{-1}) + 3i\alpha\eta'$$

$$x_2 = -\eta'^2(\kappa - 3i\alpha)(\kappa + 2i\alpha) + [\eta'(4R - 1) - \beta'](\phi - c^2\phi^{-1} + \eta') \tag{22}$$

$$x_3 = \kappa(\phi - c^2\phi^{-1}) - 2i\alpha\eta'$$

Note that when $\nu = 0$, f_1 as given here is effectively equivalent to that of *Walterscheid et al.* [1987] and *Walterscheid and Schubert* [1987] but is in a much simplified form. Without atmospheric rotation or dissipation (i.e., $c = \nu = \eta' = 0$) the dynamical factors f_1, f_2, and f_3 given in (17), (19), and (21) are numerically equivalent to those of *Walterscheid et al.* [1987], given in their equations (A1), (A2), and (A3). (Note that their equation for f_2 contains an erroneous H in the $C^2/\gamma H$ term of the denominator which should be replaced by C^2/γ.)

The system of five equations of the form of (8) for the minor species OH, O_3, H, O, and HO_2 can now be written as

$$[5 \times 5 \text{ matrix}] \begin{bmatrix} \hat{n}(\mathrm{OH}) \\ \hat{n}(\mathrm{O_3}) \\ \hat{n}(\mathrm{H}) \\ \hat{n}(\mathrm{O}) \\ \hat{n}(\mathrm{HO_2}) \end{bmatrix} = [5 \times 1 \text{ matrix}]\left(\frac{\hat{T}}{T_0}\right) \tag{23}$$

TABLE 3. Basic State Atmospheric Structure

Constituent	n_0, m^{-3}	Scale Height $= -\left(\frac{1}{n_0}\frac{dn_0}{dz}\right)^{-1}$, km
O	2.46×10^{16}	−2.8
H	2.43×10^{14}	−8.62
O_3	6.28×10^{14}	6.52
HO_2	1.23×10^{11}	1.55
$M(O_2 + N_2)$	2.37×10^{20}	5.5
O_2	4.98×10^{19}	5.5

After *Winick* [1983]. For an altitude of 83 km in the nightside model atmosphere of *Winick* [1983].

while the value of Krassovsky's ratio, η, is determined from

$$\eta = \frac{\hat{I}}{I_0}\Big/\frac{\hat{T}}{T_0} = \left\{\bar{k}_9 n_0(\mathrm{H})\hat{n}(\mathrm{O_3}) + \bar{k}_9 n_0(\mathrm{O_3})\hat{n}(\mathrm{H}) + \bar{k}_9\left(\frac{470}{T_0}\right)\frac{\hat{T}}{T_0} n_0(\mathrm{H})n_0(\mathrm{O_3}) + \bar{k}_{11} n_0(\mathrm{O})\hat{n}(\mathrm{HO_2}) + \bar{k}_{11} n_0(\mathrm{HO_2})\hat{n}(\mathrm{O})\right\} \cdot \left\{[\bar{k}_9 n_0(\mathrm{H})n_0(\mathrm{O_3}) + \bar{k}_{11} n_0(\mathrm{O})n_0(\mathrm{HO_2})]\frac{\hat{T}}{T_0}\right\}^{-1} \tag{24}$$

where the overbar denotes a time average. Equation (24) can be derived from Tables 1 and 2 by assuming that the OH nightglow intensity is directly proportional to the production rate of excited OH. The matrices appearing in equation (23) are given in Appendix 2 of *Walterscheid et al.* [1987].

RESULTS

Equation (23) was solved using a numerical matrix inversion algorithm, and then the $\hat{n}$ solution vector for the perturbation number densities of the minor constituents was used in equation (24) to obtain a value of η. The nominal basic state atmospheric parameters given in Table 3 are taken from *Walterscheid et al.* [1987] but are apparently first due to *Winick* [1983]. Other atmospheric parameters taken from the same sources are $\gamma = 1.4$ (the usual ratio of specific heats), $T_0 = 188$ K, $g = 9.8$ m s^{-1}, $R_{gas} = 0.287$ kJ kg^{-1} K^{-1} (the gas constant), $\beta = 0.21$ (the mixing ratio of molecular oxygen with respect to M), and $H(\mathrm{O}) = -2.8$ km (atomic oxygen scale height). These atmospheric parameters correspond to an altitude of maximum OH emission of about 83 km. As in the work by *Walterscheid et al.* [1987], all results are normalized with respect to $\hat{T}/T_0$, i.e., $\hat{T}/T_0 = 1$.

For all calculations involving the Coriolis force the latitude was taken to be 90° so that an upper bound for this effect was used. In spite of this, its inclusion was found to have very little influence on the overall results for this particular study at any wave period. Thus while the theory developed here allows for the inclusion of the Coriolis force, it is not incorporated in the present results. Such inclusion will be deferred to a later study.

The kinematic eddy viscosity was taken to be 200 m^2 s^{-1}, which is not an unreasonable value to use in this altitude region [*Hocking*, 1985] but which is higher than the recently inferred value of 37 m^2 s^{-1} obtained by *Gardner and Voelz* [1987] from lidar observations of gravity waves in the nighttime sodium layer. It is, however, well below values of 800–

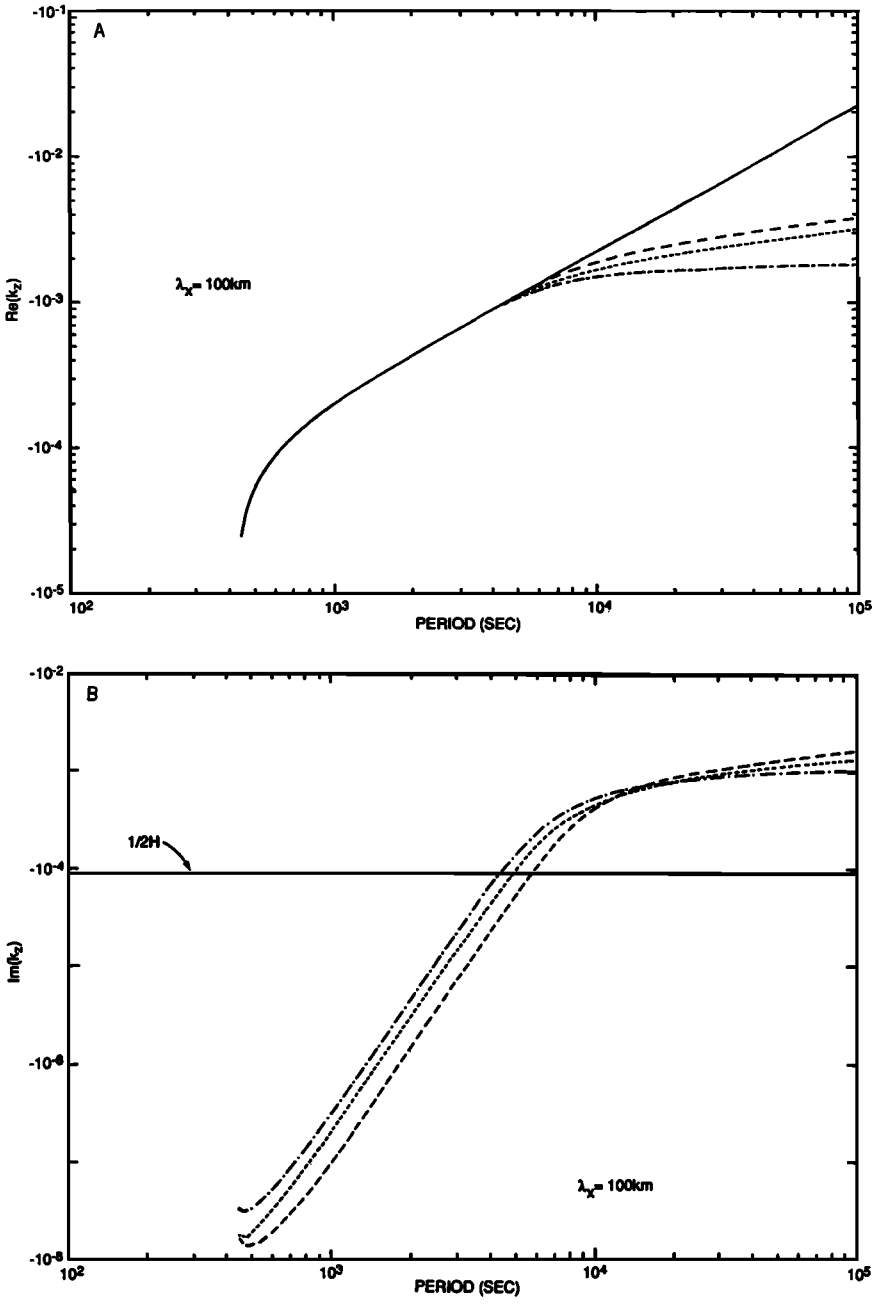

Fig. 1. (*a*) Real and (*b*) imaginary parts of the vertical wave number (k_z) versus period calculated without dissipation (solid curve), with viscosity (dotted curve), with thermal conduction (dashed curve), and with both viscosity and thermal conduction (dashed-dotted curve). Without dissipation, Im (k_z) = 0. The solid line in Figure 1*b* shows the value of $1/2H$.

8000 $m^2\ s^{-1}$ for the enhanced eddy diffusion coefficient, which were inferred from observations of breaking gravity waves in both the OH and Na layers by *Myrabo et al.* [1987]. The coefficient of eddy thermal conductivity was calculated using the same relationship as used by *Richmond and Matsushita* [1975], i.e., $\lambda = c_p\mu/2$, where c_p ($= \gamma gH/(\gamma - 1)T_0$) is the specific heat at constant pressure. From a value of total density of 1.1×10^{-5} kg m^{-3} one can deduce that $\mu = 2.2 \times 10^{-3}$ kg $m^{-1}\ s^{-1}$ and hence that $\lambda = 1.1$ kg m $s^{-3}\ K^{-1}$.

Results are confined to include only internal gravity waves having upward energy propagation. A broad range of internal gravity wave periods is considered, but all results pertain to a horizontal wavelength of 100 km. For this wavelength and for the values of atmospheric parameters considered here the transition from evanescence to propagation occurs at a period of 428.7 s (7.15 min), and so only periods greater than this are considered. For all of the results presented here the effects of chemistry are always included. Also, all of the results presented will be comparisons between those resulting from the use of the model of *Walterscheid et al.* [1987] and those from the further inclusion of either eddy viscosity, eddy thermal conduction, or both of these together.

Both the real and the imaginary parts of the vertical wave number k_z are shown as functions of wave period in Figure 1. The solid curve in Figure 1*a* is calculated using the dissipationless dispersion equation of *Hines* [1960], as was done by *Walterscheid et al.* [1987]. The other curves in this figure correspond to the inclusion of dissipation in the dispersion

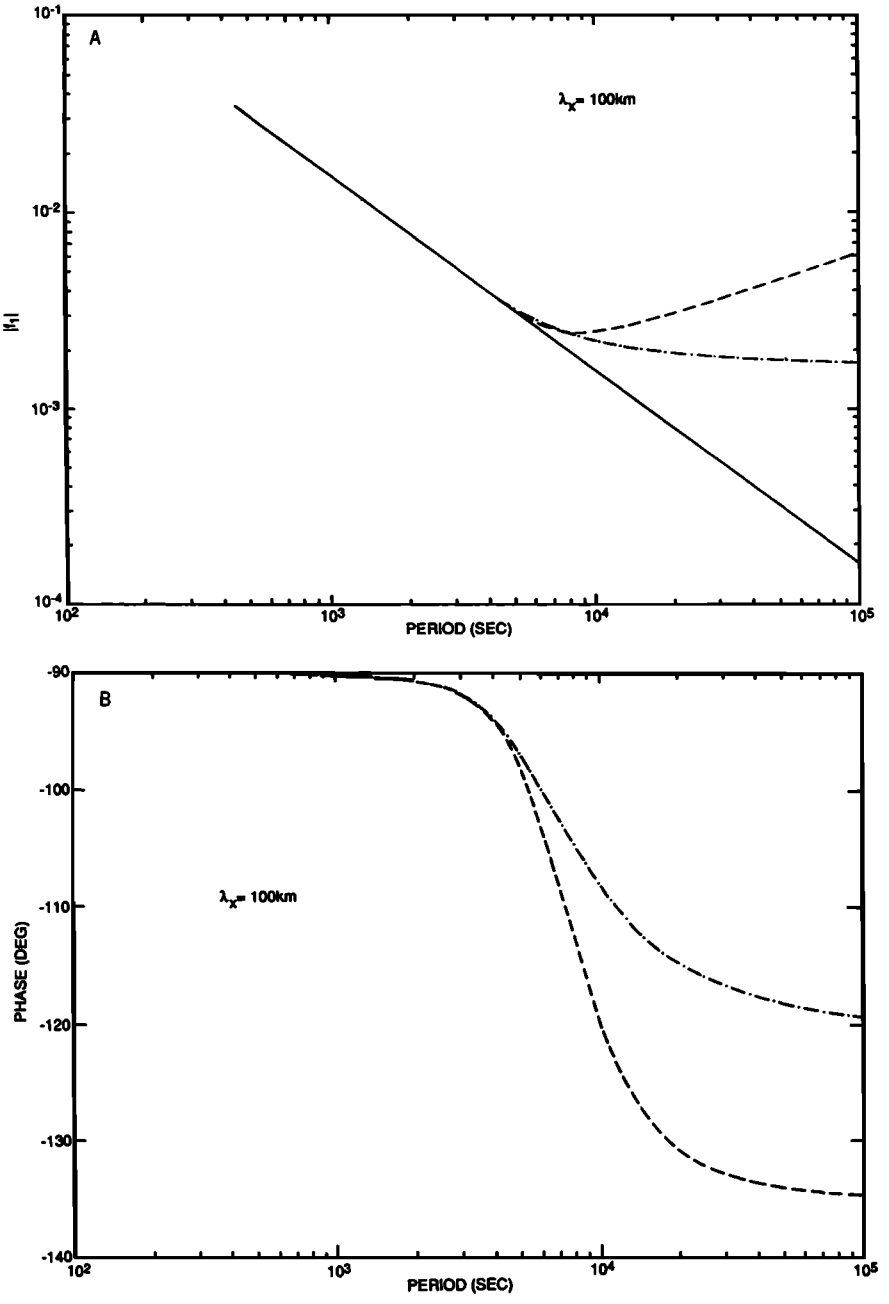

Fig. 2. (*a*) Magnitude and (*b*) phase of the dynamical factor f_1 versus period, calculated without dissipation (solid curve), with thermal conduction (dashed curve), and with both viscosity and thermal conduction (dashed-dotted curve). The case of including viscosity alone is not shown, since it has no effect on f_1. In Figure 2*b* the phase of f_1 without dissipation is $-90°$ (f_1 is purely imaginary).

equation, using the dispersion equation given by *Hickey and Cole* [1987]. Negative values of Re (k_z) correspond to upward energy propagation. One notices that the inclusion of dissipation becomes increasingly important at the longer wave periods (i.e., for the slower moving waves), as found by *Richmond* [1978] in a study of thermospheric gravity wave dissipation. One also notices that the dissipation has the effect of increasing (decreasing) the magnitude of the vertical wavelength (wave number), as found by *Klostermeyer* [1972]. The imaginary part of the vertical wave number is shown in Figure 1*b*. In the absence of any dissipation it is precisely zero, and this case corresponds to that of *Walterscheid et al.* [1987]. With dissipation it is negative, implying an energy loss in the direction of energy propagation. Once again one notices the increasing importance of dissipation at the longer wave periods. The solid line in this Figure 1*b* shows the $1/2H$ term which appears in equation (9). In the absence of dissipation the wave velocity amplitude grows with altitude as exp ($z/2H$), but dissipation suppresses this growth, particularly at the long wave periods. At periods greater than some 5000 s (1.4 hours) the wave amplitudes will be decreasing with increasing altitude due to the dominance of Im (k_z) over $1/2H$ in the exponential in equation (9).

The magnitude and phase of the dynamical factor f_1 are shown in Figures 2*a* and 2*b*, respectively. Without dissipation the magnitude of f_1 decreases linearly with increasing wave

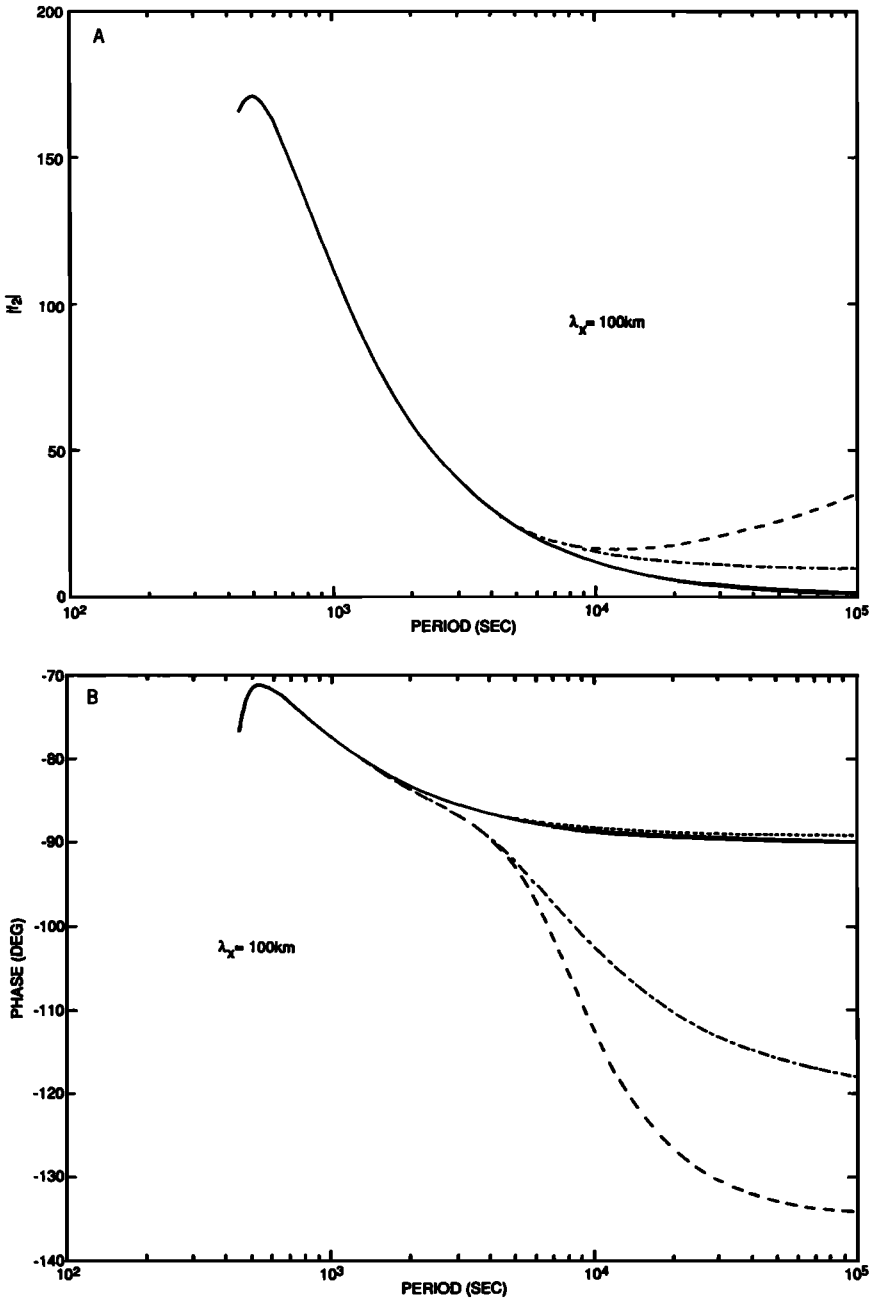

Fig. 3. (*a*) Magnitude and (*b*) phase of the dynamical factor f_2 versus period, calculated without dissipation (solid curve), with viscosity (dotted curve), with thermal conduction (dashed curve), and with both viscosity and thermal conduction (dashed-dotted curve). In Figure 3*a* the case of viscosity alone is indistinguishable from the dissipationless case.

period (Figure 2*a*). This result is unaffected by the inclusion of viscosity. However, f_1 is significantly affected by the inclusion of thermal conduction at periods greater than some 5000 s. The reason for this is that ωv is independent of ω, while R increases slowly at long periods. Hence at long periods the first term in (17) dominates. Now, with the further inclusion of viscosity, the resultant magnitude of f_1 at long periods is smaller than that obtained with only thermal conduction included. This is because the vertical wave number is smaller with both dissipative mechanisms operating, resulting in smaller values of both R and f_1. In the absence of thermal conduction, f_1 is purely imaginary, so that its phase is constant and equal to $-90°$. With the inclusion of thermal conduction the phase approaches $-135°$ at long wave periods (Figure 2*b*), while the further inclusion of viscosity sees the phase approach approximately $-119°$.

Both the magnitude (Figure 3*a*) and the phase (Figure 3*b*) of f_2 are relatively unaffected by the inclusion of the viscosity only. They are both modified at long periods by the inclusion of thermal conduction and are modified again by the further inclusion of viscosity. With both thermal conduction and viscosity operating, the magnitude of f_2 is increased several-fold at long periods, while the phase of f_2 approaches about $-118°$ at long periods compared to the dissipationless value of $-90°$.

The magnitude of f_3 (Figure 4*a*) is only slightly modified by the inclusion of dissipation. In the absence of dissipation it

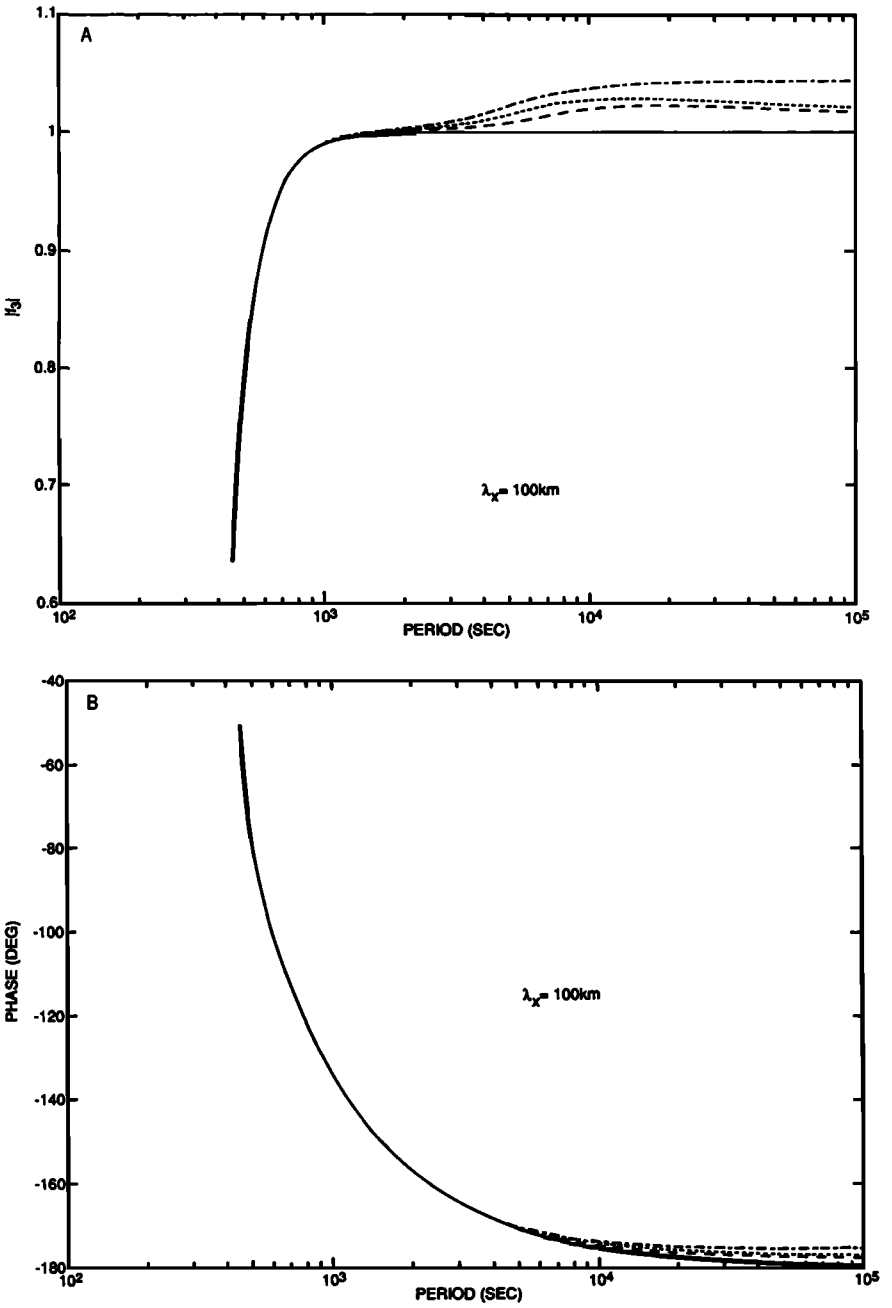

Fig. 4. As in Figure 3 but for the dynamical factor f_3.

approaches a value of unity at long periods, while with both thermal conduction and viscosity included it approaches a value of about 1.05. The phase of f_3 (Figure 4*b*) is also not significantly affected by the inclusion of dissipation. At long periods it approaches a value close to $-180°$ in the absence of dissipation and about $-175°$ with both dissipative mechanisms included. Thus the perturbation number density remains in antiphase with the perturbation temperature at long periods. This must be compared with the velocity divergence and vertical velocity, both of which lag the temperature by an increased amount due to the inclusion of the thermal conduction (and modified further by the viscosity), significantly so at the long wave periods, as evidenced by the phases of f_1 and f_2.

The values of $\hat{n}/n_0$ for each of the minor constituents are significantly affected by the inclusion of dissipation at long periods, and all are affected in much the same way. The largest modifications occur for $\hat{n}(\mathrm{OH})/n_0(\mathrm{OH})$, the magnitude of which is shown in Figure 5*a*. It is increased by a factor of about 35 at long periods by the inclusion of thermal conduction and viscosity. The phase of $\hat{n}(\mathrm{OH})/n_0(\mathrm{OH})$ is shown in Figure 5*b*. At long periods it is reduced by more than 90° by the inclusion of dissipation. The values of $\hat{n}/n_0$ for the other minor species are not shown here but are summarized in the long-period limit in Table 4.

Figures 6*a* and 6*b* show the amplitude and phase of η, respectively. With both thermal conduction and viscosity included the magnitude of η begins to depart from its nondissipative value at periods greater than some 6000 s (1.7 hours). At the very longest periods it exceeds the latter by a factor of about 20 ($|\eta| \approx 1.2$ without dissipation and 21.2 with dissi-

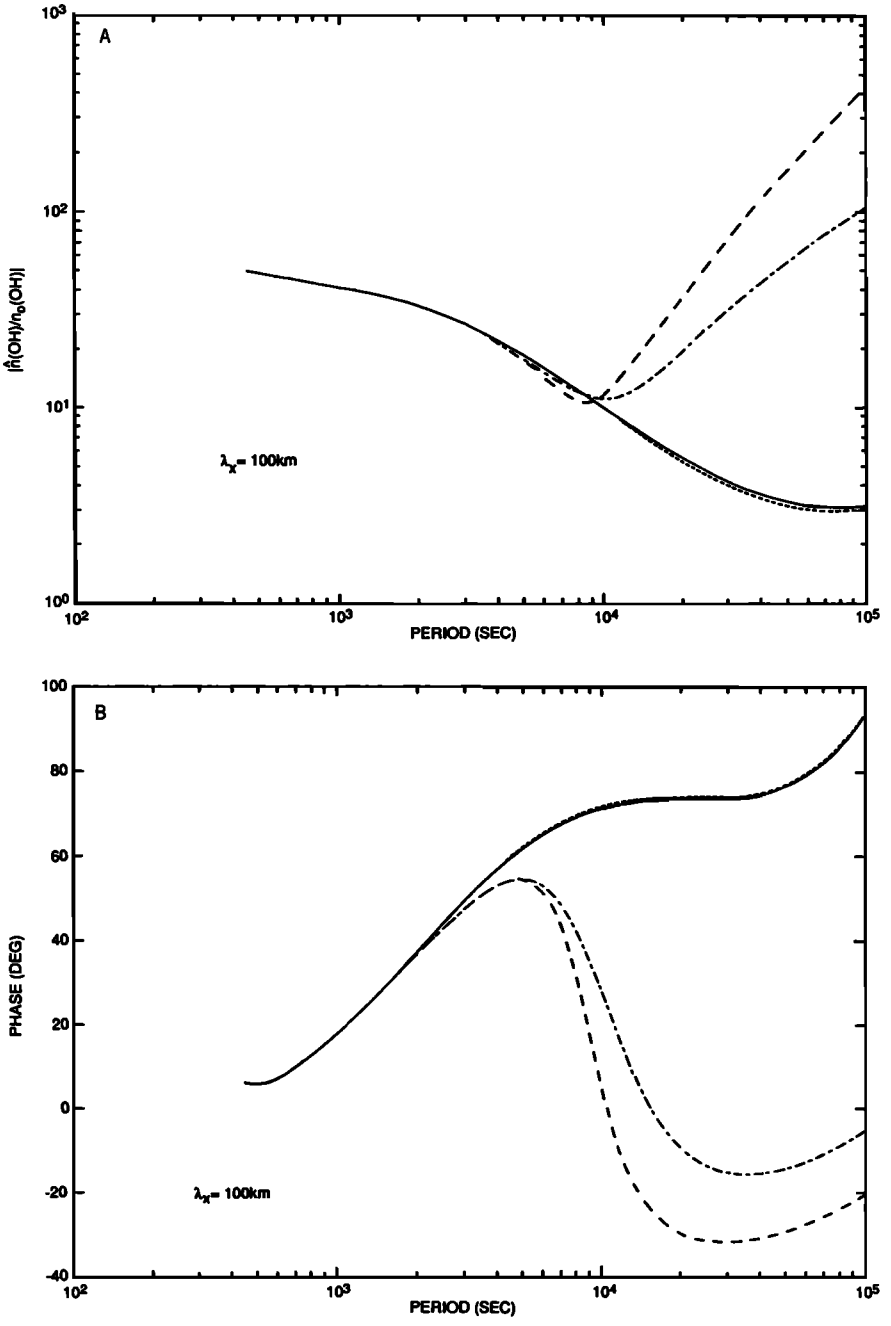

Fig. 5. Fractional concentration fluctuation $\hat{n}/n_0$(*a*) amplitude and (*b*) phase for OH versus period and normalized to $\hat{T}/T_0 = 1$: no dissipation (solid curve), with viscosity (dotted curve), with thermal conduction (dashed curve), and with both viscosity and thermal conduction (dashed-dotted curve).

pation). A change in the phase of η due to the inclusion of dissipation is apparent at periods of 3000 s (50 min). At a period of 10,000 s (2.8 hours) the dissipationless value of the phase of η leads that with dissipation included by more than 30°. In the long-period limit the phase of η without dissipation is 34.7°, while that with dissipation is only 0.8°. It is clear that one of the effects of dissipation is to bring the OH intensity fluctuations more into phase with the temperature fluctuations. It is also apparent that the phase of η is more sensitive to the inclusion of dissipation than is the magnitude of η at periods when the dissipation just begins to become important (i.e., periods of 3000–7000 s).

TABLE 4. Values of the Amplitude $|\hat{n}/n_0|$ and Phase χ of the Fractional Density Perturbations of the Minor Constituents in the Long-Period Limit (10^5/s)

	$\lvert\hat{n}/n_0\rvert$	$\lvert\hat{n}/n_0\rvert$*	χ, deg	χ,* deg
OH	3.1	105	92.6	− 5.6
O_3	6.4	34.4	174	134
H	4.7	44	0	− 28.7
O	8.3	72	16	10
HO_2	5.7	62.7	− 156	− 80.5

*Value obtained with the inclusion of both thermal conduction and viscosity.

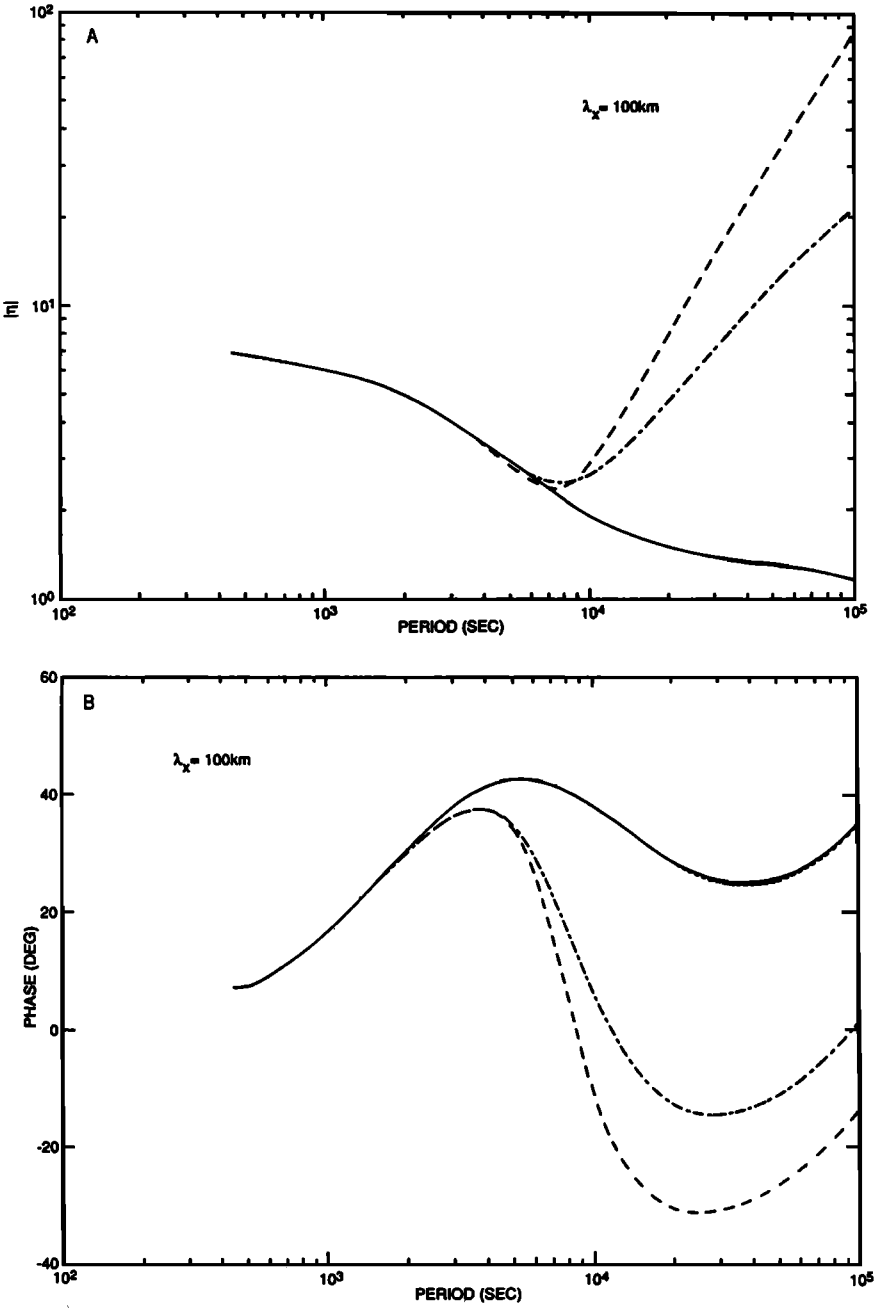

Fig. 6. (*a*) Magnitude and (*b*) phase of the ratio η of nightglow intensity fluctuations to temperature fluctuations versus period without dissipation (solid curve), with viscosity (dotted curve), with thermal conduction (dashed curve), and with both viscosity and thermal conduction (dashed-dotted curve). In Figure 6*a* the case of viscosity alone is indistinguishable from the dissipationless case and is only just discernable in Figure 6*b* at long periods.

DISCUSSION

The modification of the theory of *Walterscheid et al.* [1987] to include the effects of dissipation due to both eddy thermal conduction and viscosity (the effect of Coriolis force was also included in the theoretical development but was found to be unimportant for a wave with a 100-km horizontal wavelength), as presented here, has certain implications regarding OH observations and their interpretation. One of the effects of dissipation is to reduce wave amplitudes, more so with increasing altitude. From Figure 1*b* it is apparent that the dissipation is more severe at the longer wave periods, since |Im (k_z)| is greatest there. At the very short wave periods the wave amplitudes will be growing as $e^{z/2H}$ with increasing altitude. In between, at periods where the Im (k_z) curve intersects the $1/2H$ line (i.e., where $1/2H$ + Im $(k_z) \approx 0$), the waves are experiencing a zero amplitude growth and have in fact reached their maximum amplitudes. Hence these are the waves which are the most likely to be observed. (This and subsequent discussion takes no account of wave saturation or nonlinear effects, a subject which has been reviewed by *Fritts* [1984].) At longer wave periods the waves are experiencing severe dissipation, and their amplitudes are thus decreasing with increasing altitude. It is quite obvious, then, that these longer-period waves must have already achieved their maximum amplitudes and that this must have occurred at the lower atmospheric

levels where the dissipation rates are smaller. Because of this, the very longest period waves would not usually be easily discernable among the other waves which are present, so that one may be able to observe very large values of $|\eta|$ (see Figure 6*a*) only under extraordinary observing conditions. The generation efficiency of such waves by various sources is a subject not dealt with here but will quite obviously be a factor for any such wave observations also.

In the present study, results have been presented for a Prandtl number of 2 ($Pr = \mu c_p/\lambda$, where μ is the coefficient of viscosity, λ is the coefficient of thermal conduction, and c_p is the specific heat at constant pressure), but results to be presented elsewhere (M. P. Hickey, NASA contract report, in preparation, 1988) have investigated the consequences of increasing the Prandtl number to 10 either by increasing the eddy viscosity by a factor of 5 or by decreasing the eddy thermal conduction by a factor of 5. Increasing the eddy viscosity by a factor of 5 increases the total dissipation so that zero amplitude growth occurs for periods closer to 3000 s than the 4000 s in the $Pr = 2$ case, while $|\eta|$ begins to depart from its dissipationless value at about the same period as in the $Pr = 2$ case and at the longest periods is reduced some 30% over its $Pr = 2$ value. Decreasing the eddy thermal conduction by a factor of 5 decreases the total dissipation so that zero amplitude growth occurs for periods close to 4500 s (i.e., at periods greater than those for the $Pr = 2$ case), while $|\eta|$ begins to depart from its dissipationless value at longer periods ($\approx$8000 s) than those for the $Pr = 2$ case ($\approx$5000 s) and at the longest periods is reduced some 60% over its $Pr = 2$ value. The overall effects of increasing the Prandtl number from 2 to 10 are thus (1) to decrease the magnitude of η at the longest wave periods (though the associated values of $|\eta|$ are still significantly greater than their dissipationless counterparts) and (2) to increase the separation between the periods where maximum wave amplitudes are occurring (as defined by the zero-amplitude growth condition) and the periods where modifications to the values of $|\eta|$ as a consequence of eddy dissipation are occurring. Thus observations of values of η which have been noticeably modified by eddy dissipation are more likely to be made when the associated Prandtl numbers are small. *Fritts and Dunkerton* [1985] have shown that turbulent Prandtl numbers associated with convectively unstable gravity waves may achieve large values over limited regions of altitude within the mesosphere. This suggests that one may find it more difficult to measure values of η which have been noticeably modified by eddy dissipation in a more turbulent mesosphere, provided that the increased turbulence is due to convectively unstable gravity waves. Mesospheric turbulence is strongest at the solstices and weakest at the equinoxes [e.g., *Garcia and Solomon*, 1985], so that consequently observed values of η may be seasonally dependent.

Sivjee et al. [1987] and *Hecht et al.* [1987] have compared observed values of η with those obtained using the model of *Walterscheid et al.* [1987] for waves of periods of hours or more. The plausibility of the association of the observations with theory was established, and it was found that at times in order to obtain best agreement between the two it was necessary to assume that the OH layer peaked at 87 km (and not 83 km), or that the atomic oxygen scale height (H(O)) was different from -2.8 km (either -2.0 km or -4.0 km), or that both of these assumptions were required together. The effect of decreasing H(O) is to increase $|\eta|$ and decrease the phase of η, while the effect of raising the emission layer to 87 km is to decrease both $|\eta|$ and phase of η (see Figures 5 and 7, respectively, of *Walterscheid et al.* [1987]). Since the inclusion of dissipation modifies the value of η at periods of hours, as evidenced in Figures 6*a* and 6*b*, it is clear that a true comparison between observation and theory will require, at times, the inclusion of dissipation.

The behavior of η calculated with the inclusion of eddy dissipation has certain features about it which have been observed in gravity wave driven fluctuations in the OH nightglow at Poker Flat (R. Viereck, private communication, 1987). These include a general decrease in $|\eta|$ with increasing wave period toward a minimum in $|\eta|$ (which occurs somewhere between 10^3 and 10^4 s) and thereafter an increase in $|\eta|$ with increasing period, and a tendency for the phase of η to be less than or equal to 0° at long periods. This demonstrates the need to include eddy dissipation in the gravity wave dynamics in order to properly describe the behavior of η at periods of hours.

The dissipationless theory of *Walterscheid et al.* [1987] also demonstrated that at gravity wave periods of hours, η was insensitive to changes in the horizontal wavelength (λ_x) of the waves (see their Figures 4*a* and 4*b*). This further simplified any comparisons which were to be made between observations and theory (as, for example, in the work by *Sivjee et al.* [1987] and *Hecht et al.* [1987]) because it meant that the horizontal wavelengths of the observed waves did not need to be known in order to calculate η from the theoretical model. However, a quick glance at the thermal conduction parameter ν in equation (15) reveals it to be proportional to k_x^2 (i.e., $\nu \propto \lambda_x^{-2}$), which automatically places a λ_x dependence on the dynamical factors f_1, f_2, and f_3 and hence also on η. Results of calculations investigating the dependence of η on λ_x with the inclusion of dissipation has been presented elsewhere [*Hickey*, 1988], but it is simply stated here that its inclusion is unlikely to be very important for horizontal wavelengths of 1000 km or more (bearing in mind that the inclusion of viscosity alone had no significant effect on the results). This implies that one cannot a priori preclude the effects of dissipation without first having some estimate of the horizontal wavelength. This could be achieved simply by using a system of three spaced spectrometers to make the OH observations or, as was done by *Myrabo et al.* [1987], by also making observations of the Na layer using a lidar system in order to estimate the vertical wavelengths, from which limits on the horizontal wavelengths can be derived.

Walterscheid et al. [1987] find that the linear treatment of the fluctuation dynamics should remain valid for relative temperature fluctuations approaching 20%. With the inclusion of dissipation the relative density fluctuations of the minor species are very large at the longest of wave periods, and it would appear that then the linear treatment may not be valid. However, at these longest wave periods the dissipation will limit the magnitude of the temperature fluctuations so that a linear treatment may still be valid.

The effects of background winds have not been included here but have been discussed briefly by *Hecht et al.* [1987]. The winds will Doppler shift the wave frequencies, increasingly so for the waves of smaller horizontal phase trace speed (i.e., for long periods, short horizontal wavelengths). For such waves, observed values of η will differ from model predictions so that at times the effect of winds may need to be included in the models, and the azimuth of phase propagation as well as the horizontal wavelengths will then need to be known. In the

vicinity of a critical level the winds will cause a Doppler shifting of the wave frequency to a value close to zero, so that in this instance, large values of η may be observed. Relative temperature perturbations associated with gravity waves increase in a small region just below a critical level [*Bowman et al.*, 1980], and because the values of η calculated here were normalized to the relative temperature perturbations, the relative intensity perturbations should also increase just below a critical level.

All of the foregoing theory has assumed the emission to occur at a single level in the atmosphere, whereas the emission layer is several kilometers thick. Thus interference between emissions from different levels will become important for those waves having vertical wavelengths less than or comparable to the thickness of the emitting layer, as demonstrated by *Hines and Tarasick* [1987] and by G. Schubert and R. L. Walterscheid (Wave-driven fluctuations in OH nightglow from an extended source region, paper submitted to *Journal of Geophysical Research*, 1987). In particular, the study of Schubert and Walterscheid shows that for short vertical wavelengths, interference effects cause a large reduction in the airglow intensity, implying an observational bias toward those waves of larger vertical wavelength. Since the eddy dissipation included here is most important at the shorter vertical wavelengths (corresponding to the longer periods in Figure 6), the results presented here would be modified further by performing an integration over the whole emitting layer. Likewise, the results of Schubert and Walterscheid would be modified further by the inclusion of eddy dissipation because the effect of dissipation at short vertical wavelengths is to increase the vertical wavelengths over their nondissipative values, thus modifying the interference effects. Obviously, a complete theory must include all of these effects together in order that a useful comparison with observations can be performed. Nonetheless, as stated previously, the observations of R. Viereck (private communication, 1987) show similar characteristics in η to those of the results presented here.

CONCLUSION

The model of *Walterscheid et al.* [1987] has been modified to include in the gravity wave dynamics the effects of dissipation due to eddy thermal conduction and viscosity as well as the Coriolis force by employing the shallow atmosphere approximation. For the nominal case considered here the Coriolis force was found to be unimportant at any wave period. The inclusion of the thermal conduction alone greatly modified the results at long wave periods, while the inclusion of the viscosity alone had a negligible effect at any period. However, when the viscosity was included in conjunction with the thermal conduction, the results were changed significantly from those which only included the thermal conduction.

The effect of dissipation is to bring the OH intensity fluctuations more into phase with the temperature fluctuation (i.e., decrease the phase of η) and to increase the magnitude of the intensity fluctuations relative to the temperature fluctuations (i.e., increase $|\eta|$). The phase of η appears to be more sensitive to the inclusion of dissipation than is the magnitude of η at periods when the dissipation just begins to become important.

The wave dissipation was found to be the most severe at the very longest of wave periods, which in the real atmosphere will place an observational constraint on such waves. These waves, with their associated very high values of $|\eta|$, are unlikely to be often observed. However, as the wave periods are decreased ($|\eta|$ will decrease too), the probability of observing the waves will be increased (i.e., as one approaches the wave period regime where the waves are achieving maximum amplitudes), so that there will be times when waves are being observed which have associated with them values of η which have been modified by dissipation.

The inclusion of dissipation in the gravity wave dynamics effectively places a strong horizontal wavelength dependence on η which does not exist in the dissipationless theory. This may have implications regarding comparisons made between observation and theory and will mean that at times the horizontal wavelengths of the waves will need to be known. Work exploring the dependence of η on horizontal wavelength can be found in the paper by *Hickey* [1988].

Acknowledgments. I would like to thank S. A. Smith for his many helpful comments made during the preparation of this paper, and R. Viereck for making available to me some of his data before they were published. This paper has benefited from the comments of its reviewers. This work was supported by NASA contract NAS8-36400.

The Editor thanks C. Deehr and R. L. Walterscheid for their assistance in evaluating this paper.

REFERENCES

Bowman, M. R., L. Thomas, and R. H. Thomas, The propagation of gravity waves through a critical layer for conditions of moderate wind shear, *Planet. Space Sci.*, *28*, 119–133, 1980.

Ebel, A., Contributions of gravity waves to the momentum, heat, and turbulent energy budget of the upper mesosphere and lower thermosphere, *J. Atmos. Terr. Phys.*, *46*, 727–737, 1984.

Fritts, D. C., Gravity wave saturation in the middle atmosphere: A review of theory and observations, *Rev. Geophys.*, *22*, 275–308, 1984.

Fritts, D. C., and T. J. Dunkerton, Fluxes of heat and constituents due to convectively unstable gravity waves, *J. Atmos. Sci.*, *42*, 549–556, 1985.

Garcia, R. R., and S. Solomon, The effect of breaking gravity waves on the dynamics and chemical composition of the mesosphere and lower thermosphere, *J. Geophys. Res.*, *90*, 3850–3868, 1985.

Gardner, C. S., and D. G. Voelz, Lidar studies of the nighttime sodium layer over Urbana, Illinois, 2, Gravity waves, *J. Geophys. Res.*, *92*, 4673–4694, 1987.

Hecht, J. H., R. L. Walterscheid, G. G. Sivjee, A. B. Christensen, and J. B. Pranke, Observations of wave-driven fluctuations of OH nightglow emission from Sondre Stromfjord, Greenland, *J. Geophys. Res.*, *92*, 6091–6099, 1987.

Hickey, M. P., Wavelength dependence of eddy dissipation and Coriolis force in the dynamics of gravity wave driven fluctuations in the OH nightglow, *J. Geophys. Res.*, this issue, 1988.

Hickey, M. P., and K. D. Cole, A quartic dispersion equation for internal gravity waves in the thermosphere, *J. Atmos. Terr. Phys.*, *49*, 889–899, 1987.

Hines, C. O., Internal atmospheric gravity waves at ionospheric heights, *Can. J. Phys.*, *38*, 1441–1481, 1960.

Hines, C. O., and D. W. Tarasick, On the detection and utilization of gravity waves in airglow studies, *Planet. Space Sci.*, *35*, 851–866, 1987.

Hocking, W. K., Turbulence in the altitude region 80–120 km, *Handb. Middle Atmos. Program*, *16*, 290–304, 1985.

Klostermeyer, J., Influence of viscosity, thermal conduction, and ion drag on the propagation of atmospheric gravity waves in the thermosphere, *Z. Geophys.*, *38*, 881–890, 1972.

Krassovsky, V. I., Infrasonic variations of OH emission in the upper atmosphere, *Ann. Geophys.*, *28*, 739–746, 1972.

Myrabo, H. K., C. S. Deehr, and R. Viereck, Polar mesopause gravity wave activity in the sodium and hydroxyl night airglow, *J. Geophys. Res.*, *92*, 2527–2534, 1987.

Richmond, A. D., Gravity wave generation, propagation and dissipation in the thermosphere, *J. Geophys. Res.*, *83*, 4131–4145, 1978.

Richmond, A. D., and S. Matsushita, Thermospheric response to a magnetic substorm, *J. Geophys. Res.*, *80*, 2839–2850, 1975.

Schoeberl, M. R., D. F. Strobel, and J. P. Apruzese, A numerical

model of gravity wave breaking and stress in the mesosphere, *J. Geophys. Res.*, *88*, 5249–5259, 1983.

Sivjee, G. G., R. L. Walterscheid, J. H. Hecht, R. M. Hamwey, G. Schubert, and A. B. Christensen, Effects of atmospheric disturbances on polar mesopause airglow OH emissions, *J. Geophys. Res.*, *92*, 7651–7656, 1987.

Smith, S. A., D. C. Fritts, B. B. Balsley, and C. R. Philbrick, Simultaneous rocket and MST radar observation of an internal gravity wave breaking in the mesosphere, *Handb. Middle Atmos. Program*, *20*, 136–146, 1986.

Walterscheid, R. L., Dynamical cooling induced by dissipating internal gravity waves, *Geophys. Res. Lett.*, *8*, 1235–1238, 1981.

Walterscheid, R. L., and G. Schubert, A dynamical-chemical model of tidally driven fluctuations in the OH nightglow, *J. Geophys. Res.*, *92*, 8775–8780, 1987.

Walterscheid, R. L., G. G. Sivjee, G. Schubert, and R. M. Hamwey, Large-amplitude semidiurnal temperature variations in the polar mesopause: evidence of a pseudotide, *Nature*, *324*, 347–349, 1986.

Walterscheid, R. L., G. Schubert, and J. M. Straus, A dynamical-chemical model of wave-driven fluctuations in the OH nightglow, *J. Geophys. Res.*, *92*, 1241–1254, 1987.

Weinstock, J., Gravity wave saturation and eddy diffusion in the middle atmosphere, *J. Atmos. Terr. Phys.*, *46*, 1069–1082, 1984.

Winick, J. R., Photochemical processes in the mesosphere and lower thermosphere, in *Solar-Terrestrial Physics*, edited by R. L. Carovillano and J. M. Forbes, pp. 677–732, D. Reidel, Hingham, Mass., 1983.

M. P. Hickey, Universities Space Research Association, NASA Marshall Space Flight Center, ED-44, Huntsville, AL 35812.

(Received June 29, 1987;
revised December 10, 1987;
accepted December 11, 1987.)